

SYNTHESIS, GROWTH, STRUCTURAL, SPECTRAL, THERMAL AND DIELECTRIC STUDIES OF A NEW ORGANIC SALT CRYSTAL: 2- AMINO - 5- CHLOROPYRIDINIUM PYRIDINE- 2- CARBOXYLATE MONOHYDRATE

T. JAYANALINA*, G. RAJARAJAN, K. BOOPATHI

Department of Physics, K.S.R.College of Engineering, Tiruchengode 637215, Tamil Nadu, India

Department of Physics, Vidhya Mandhir Institute of Technology, Erode 638052, Tamil Nadu, India

Centre for Crystal Growth, SSN College of Engineering, Kalavakkam, Chennai 603110, Tamil Nadu, India

Single crystals of 2- amino - 5- chloropyridinium pyridine- 2- carboxylate monohydrate [abbreviated as 2A5CPC] were grown using slow solvent evaporation method. The structure of the grown crystals was confirmed by single crystal X- ray diffraction (SCXRD) technique. The H^1 NMR and C^{13} NMR spectra were recorded to elucidate the molecular structure of the grown crystal. The presence of functional groups was ascertained by Fourier transform infrared analysis. The optical properties of the crystals were investigated by UV-Vis-NIR transmission spectra and the band gap of the grown crystal was determined as 5.25 eV. The dielectric measurements of the grown crystal were carried out with different frequencies and temperatures. Vickers micro hardness measurement was carried out to study the mechanical behavior of the grown crystal. The surface morphology and elemental prediction of the grown crystal were analyzed using SEM and EDAX analysis.

(Received August 4, 2015; Accepted October 9, 2015)

Keywords: Crystal growth, Molecular structure, X- ray technique, Thermal behavior and Surface morphology

1. Introduction

In recent years, search for organic single crystal in the application of telecommunication, frequency doubling and optoelectronics had been increased considerably [1-5]. This is because of their efficient physiochemical properties such as molecular nonlinearity over a broad frequency range, low cost, inherent synthetic flexibility, high optical damage threshold ($> 10\text{GW}/\text{cm}^2$), ultrafast response with better process ability, ease of fabrication and possible integration into devices. Researchers are giving an appreciable attention to grow organic single crystals for technological applications. The crystalline organic materials allow one to fine tune their optical properties through molecular engineering and chemical synthesis [6]. More than 70% of organic compounds crystalline in centrosymmetric space group due to the predominant anti-parallel π -stacking between the aromatic rings as a consequence of dipolar interactions [7, 8]. Organic crystals offer flexibility in molecular design [9]. Pyridine is a heterocyclic organic compound with the chemical formula C_5H_5N . Intensive studies on pyridine and pyridine derivatives have been made in the past, keeping in the view of their industrial importance both as fundamental building block and reagent in organic synthesis. Some of the reported promising 2- amino pyridine derivatives are 2-amino-5-chloropyridinium-L-tartrate (2A5CPLTA) [10], 2-amino-5-nitropyridinium dihydrogen phosphate, 2-amino-5-nitropyridinium dihydrogen arsenate, 2-amino-5-nitropyridinium acetophosphate, 2-amino-5-nitropyridinium chloride (2A5NPCl), 2-amino-5-nitropyridinium bromide (2A5NPBr) and 2-amino-5-nitropyridinium- L-monohydrate tartrate

*Corresponding author: jayanalina@gmail.com

(2A5NPLT)[11- 13]. Picolinic acid, an isomer of nicotinic acid is used as an intermediate to produce pharmaceuticals (especially local anesthetics) and metal salts for the application of nutritional supplements. This organic material crystallizes in the monoclinic crystal system with centrosymmetric space group $P 2_1/c$, and the unit cell parameters are $a = 9.1868(7)\text{\AA}$, $b = 19.3639(13)\text{\AA}$, $c = 14.6336(11)\text{\AA}$. The crystal structure consists of 2-amino-5-chloropyridinium and picolinic acid molecules held together by a network of hydrogen bonds resulting in two-dimensional hydrogen bond framework.

Single crystals of 2A5CPC in reasonable size are grown from solution of 2A5CPC by slow evaporation technique. In the present investigation, structural, crystal growth, spectral, optical, thermal, mechanical, dielectric, surface morphology and elemental prediction have been reported for the first time.

2. Experimental procedure

2.1 Synthesis, Solubility and crystal growth

The title compound was synthesized by taking 2-amino-5-chloropyridine (Sigma-Aldrich 99 %) and 2- picolinic acid (Merck 99 %) in an equimolar ratio. The calculated amount of 2-amino- 5- chloropyridine was first dissolved in methanol. 2- picolinic acid was dissolved in double distilled water and then added to the solution slowly by stirring. To obtain the homogenous solution it was continuously stirred for 6 hours and filtered using Whatman filter paper. This filtered solution was allowed to dry at room temperature and the salts were obtained. The dried salt was collected and used for the further growth of 2A5CPC crystal. The purity of the synthesized salt was further improved by successive recrystallization process.

The solubility of 2- amino - 5- chloropyridinium pyridine- 2- carboxylate monohydrate was assessed using methanol as a solvent at different temperatures ranging from 25-50 °C. The amount of 2A5CPC required to make the saturated solution at different temperatures was estimated gravimetrically and the obtained solubility curve of 2A5CPC is shown in Fig.1. From the solubility study, it is found that the title compound exhibits positive solubility in methanol solvent.

The saturated solution of 2A5CPC was prepared at room temperature in accordance with the solubility data. The saturated solution was filtered using Whatman filter paper of porosity 0.1 μm . The filtered solution was placed in the 300 ml beaker and tightly covered with perforated sheets to allow it to get crystallized by the slow evaporation technique. Single crystals of 2A5CPC were obtained after 30 days by slow evaporation method and the photograph of the grown crystal is shown in Fig.2. Good quality single crystals were extracted for characterization studies.

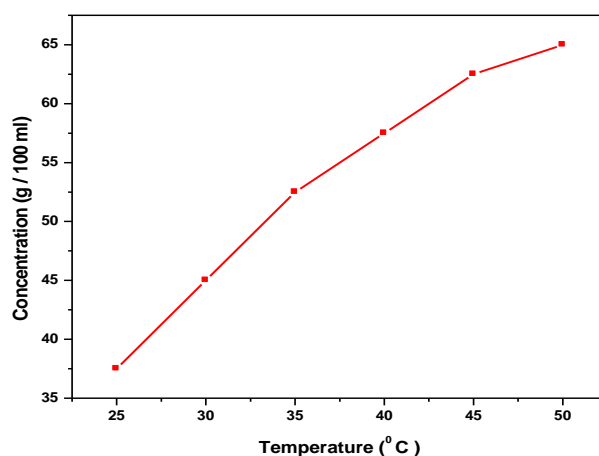


Fig.1. Solubility Curve of 2A5CPC

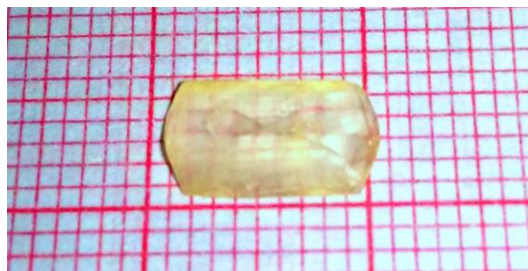


Fig.2. As grown single crystal of 2A5CPC

3. Results and discussion

3.1 Single crystal X-ray diffraction studies

The single crystal X-ray diffraction studies of 2A5CPC were performed using Bruker AXS Kappa APEX II CCD diffractometer equipped with graphite monochromated Mo K α radiation (λ 0.71073 Å) at room temperature. The single crystal of size 0.35×0.30×0.20 mm³ was used for the study. Accurate unit cell parameters were determined from the reflections of 36 frames measured in three different crystallographic zones by the method of difference vectors. Data collection, data reduction and absorption correction were performed by APEX2, SAINT-plus and SADABS programs[14]. A total of 12691 reflections were recorded with 2 θ range from 1.79 to 28.18 of which 2688 reflections are considered as unique reflections with $I > 2\sigma(I)$. The structure was solved by direct method procedure using SHELXS-97 program and refined by Full-matrix least squares procedure on F^2 using SHELXL-97 program[15]. The final refinement converges to R-values of $R_1 = 0.1556$ and $WR_2 = 0.1976$. The crystallographic data and the refinement details for 2A5CPC are summarized in Table 1. Fig.3 shows the ORTEP plot of the molecule drawn at 50% probability thermal displacement ellipsoids with the atom numbering scheme. All the hydrogen atoms were positioned geometrically [C–H = 0.93 Å–0.96 Å, N–H = 0.86 Å–0.88 Å] and were refined. The asymmetric unit of the title compound consists of a neutral 2-amino-5-chloropyridine molecule and a half of the 2-picolinic acid molecule which lies on an inversion center. The dihedral angle between the pyridine ring and the plane formed by the 2-picolinic acid is 72.31(8) Å. In the title compound the bond distances of C–C in the aromatic ring ranges from 1.348 (4) to 1.397(4) Å, with the average being 1.372 Å. The bond distance, C(16)–C(17) [1.342 (5) Å] is slightly shorter compared with other C–C distances in the ring. This shortening may be due to the effect of N3 attached to C(17). The C(13)–C(14) and C(15)–C(16) distances are larger than the other C–C bonds and their values are 1.404(4) Å and 1.403(5) Å. The bond distances of the carbon atoms in 2-picolinic acid are C(11)–C(10)–C(9) and C(3)–C(2)–C(1) are 118.7 (4) Å and 120.4(3) Å respectively. In the 2-picolinic acid molecule there is a short intermolecular O–H...O contact. In the crystal, the 2-picolinic acid molecules are linked via pairs of O–H...O hydrogen bonds, forming inversion dimers. These dimers are linked via number of O–H...O and N–H...O hydrogen bonds involving the two components, forming a three-dimensional network. The 2-amino-5-chloropyridine molecules interact with the carboxyl group of 2-picolinic acid molecule through N–H...O and O–H...N hydrogen bonds forming centrosymmetric $R_2^2(8)$ ring motifs into a two-dimensional network parallel to (100). The hydrogen bond is the most important of all directional intermolecular interactions. The corresponding data for the H-bonds are listed in Table 2.

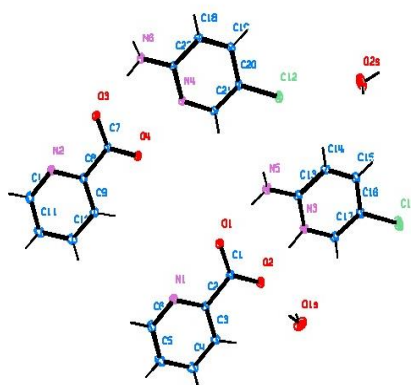


Fig. 3ORTEP plot of 2A5CPC

Table1. Crystal data and structural refinement of 2A5CPCcrystal

Empirical formula	C11 H12 Cl N3 O3
Formula weight	269.69
Temperature	296(2) K
Wavelength	0.71073 Å
Crystal system, space group	Monoclinic, P2 ₁ /c
Unit cell dimensions	a = 9.1868(7) Å alpha = 90 deg. b = 19.3639(13)Å beta = 106.824(4)deg. c = 14.6336(11)Å gamma = 90 deg..
Volume	2491.8(3) Å ³
Z, Calculated density	8, 1.438 Mg/m ³
Absorption coefficient	0.311mm ⁻¹
F(000)	1120
Crystal size	0.35 x 0.30 x 0.20 mm
Theta range for data collection	1.79 to 28.18 deg
Limiting indices	-10<=h<=12, -25<=k<=20, -19<=l<=12
Reflections collected / unique	12691 / 5960 [R(int) = 0.0599]
Completeness to theta = 28.16	97.2 %
Absorption correction	Semi-empirical from equivalents
Max. and min. transmission	0.9404 and 0.8990
Refinement method	Full-matrix least-squares on F ²
Data / restraints / parameters	5960 / 12 / 361
Goodness-of-fit on F ²	0.904
Final R indices [I>2sigma(I)]	R1 = 0.0579, wR2 = 0.1401
R indices (all data)	R1 = 0.1557, wR2 = 0.1976
Largest diff. peak and hole	0.364 and -0.374 e.Å ⁻³

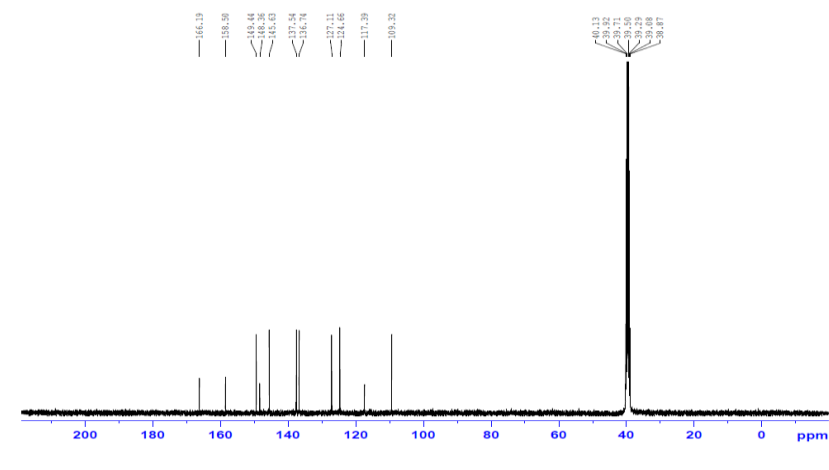


Fig. 4. (b) ^{13}C NMR spectrum of 2A5CPC

3.3 Fourier Transform Infrared (FTIR) spectral analysis

The FT-IR spectrum of 2A5CPC has been recorded in the range of $400\text{--}4000\text{cm}^{-1}$ employing Perkin- Elmer spectrometer by KBr pellet method in order to study the presence of various functional groups. Fig.5 shows the FT-IR spectrum of the grown 2A5CPCcrystal. From the spectrum, the sharp peak appears at 3484 cm^{-1} is due to the N-H stretching. The symmetric stretching of C-H is observed at 2730 cm^{-1} . The peak at 1680 cm^{-1} corresponds to the asymmetric modes of carboxylate anion (COO^-). The absorption peak at 1492 cm^{-1} region is due to symmetrical N-H stretching vibrations. The N-H bending of primary amine is observed at 1553 cm^{-1} . The peak at 1620 cm^{-1} corresponds to C= O vibration. The peaks at 1338 cm^{-1} & 891 cm^{-1} are due to the deformation of OH stretching. The C-N stretching appears at 1249 cm^{-1} . The peak at 742 cm^{-1} is assigned to C-Cl stretching. The peak at 988 cm^{-1} corresponds to C-C symmetric vibration. The C-H deformation is observed at 659 cm^{-1} . The observed vibrational frequencies and their assignment are listed in Table 3.

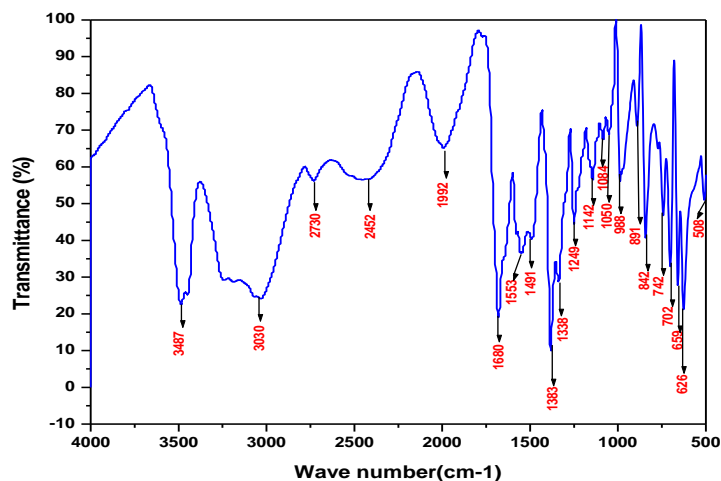


Fig. 5 FT- IR spectrum of 2A5CPC

Table3. FT-IR frequency assignments of 2A5CPCcrystal

Wave number (cm ⁻¹)	Assignments
3487	N-H stretching
2730	Symmetric stretching of C-H
1680	Asymmetric modes of carboxylate anion (COO ⁻)
1553	N- H bending of primary amine
1620	C=O vibration
1492	Symmetric stretching of N-H
1338	Stretching of the OH deformation
1249	Stretching of C-N
988	C- C symmetric vibration
891	Stretching of the OH deformation
742	C-Cl stretching
659	C- H deformation

3.4 UV-vis-NIR spectral analysis

The UV-vis-NIR spectrum is studied by Perkin Elmer Lambda 35 spectrometer with a 2A5CPC single crystal of 2mm thickness in the range of 200–1000 nm. These studies were carried out without any antireflection coatings. It reveals that grown crystal has wide transmission in the entire range without any absorption peak. The recorded transmittance spectrum is shown in Fig.6 (a) . The lower cutoff wavelength is 225nm and the crystal is found to be transparent in the region of 300- 1000 nm, which suggests the suitability of the grown crystal for various optical applications. The optical band gap of the crystal was evaluated (Fig. 6 (b)) by plotting $(\alpha h\nu)^2$ versus $h\nu$ and it was found to be 5.25 eV. The wide band gap of the 2A5CPC crystals confirms the large transmittance in the visible region and also confirms the defect concentration is less in the grown crystal [16].

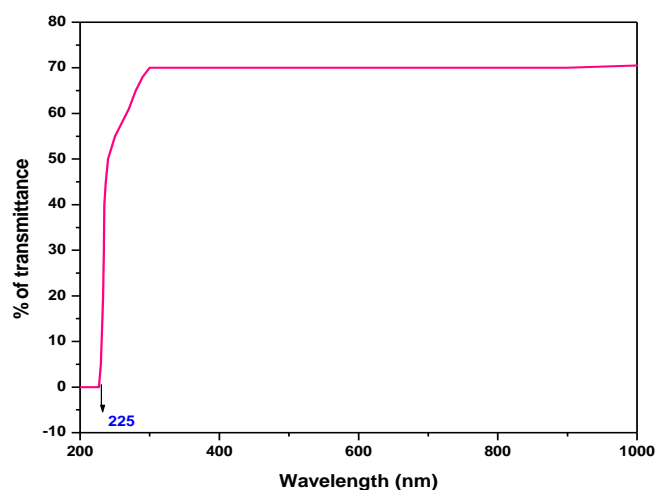


Fig.6 (a) UV- visible-NIR transmittance spectrum

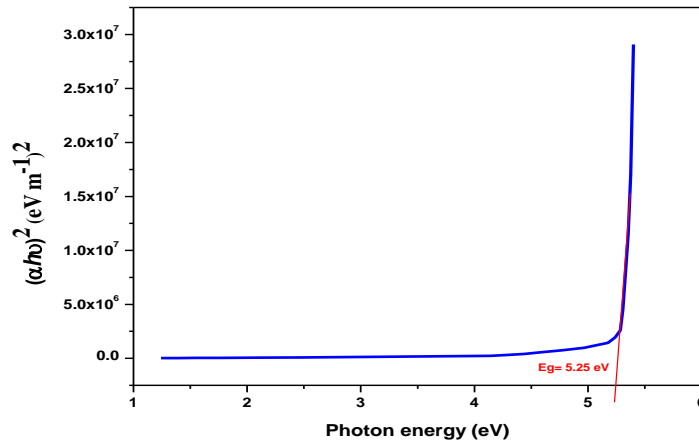


Fig.6 (b) Plot of $(ah\nu)^2$ versus photon energy

3.5 Dielectric studies

The dielectric measurements were carried out on the grown 2A5CPC single crystal with respect to the temperature and frequency. Practically, the presence of a dielectric between the plates of a condenser enhances the capacitance. Essentially, dielectric permittivity ϵ is the measure of how easily a material is polarized in an external electric field [17]. The dielectric behavior was measured using Agilent 4284-A LCR meter. Using LCR meter, the capacitance of crystal was measured for the frequencies 1, 10 and 100 kHz at various temperatures. The dielectric permittivity of the crystals was calculated using the relation $\epsilon_r = Cd/\epsilon_0 A$ where ϵ is the permittivity of free space, t is the thickness, C capacitance and A is area of cross section of the sample. It is clear from Fig. 7 (a) the dielectric permittivity observed for 2A5CPC crystal. The dielectric permittivity of a material is generally composed of four types of contributions, viz., ionic, electronic, orientation and space charge polarizations, which depend on the frequencies. At higher frequencies the decreased dielectric permittivity value could be due to the reduction in the space charge polarization. The space charge polarization will depend on the purity and perfection of the material, and its influence is large at high temperatures. The low value of dielectric values, at high frequencies indicates the low power dissipation and the crystal can be highly suitable for electro-optic applications. Fig. 7 (b) illustrates the dielectric loss of the grown crystal, the loss of energy that goes into heating a dielectric material in a varying electric field. The behavior of low dielectric loss with high frequency for the sample suggests that the crystal possesses enhanced optical quality with lesser defects and this parameter plays a vital role for the fabrication of nonlinear optical devices [18].

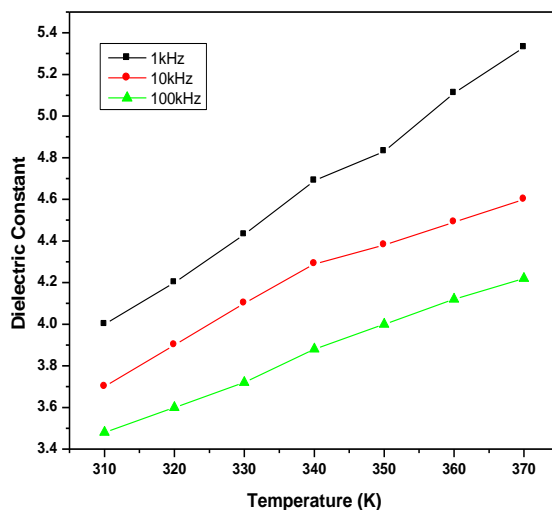


Fig. 7(a). Plot of dielectric permittivity Vs temperature for 2A5CPC

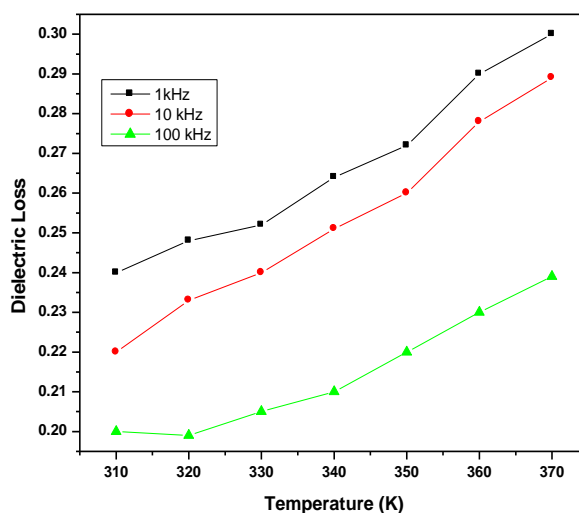


Fig.7 (b) Plot of dielectric loss Vs temperature for 2A5CPC

3.6 Micro hardness

Micro hardness measurement was carried out using Leitz Wetzlar Vickers micro hardness tester fitted with a diamond pyramidal indenter attached to an optical microscope. The micro hardness value was calculated using following relation.

$$H_V = 1.8544 (P/d^2) \text{ kg/mm}^2$$

where H_V is the Vickers hardness number, P is the applied load and d is the diagonal length of the indentation. Fig. 8(a) shows the variation of H_V as a function of applied load ranging from 20g to 80g for 2A5CPC crystal. It is observed that H_V increases with the increase of load, which indicates the reverse indentation size effect (RISE). The cracks have been observed beyond 75g for 2A5CPC. This type of variation of hardness with load is termed as reverse indentation size effect [19]. At low loads, the indenter penetrates only the top surface layers generating dislocations, which results in the increase of hardness in this region. The load independence of hardness at

higher loads can be attributed to the mutual interaction or rearrangement of dislocations. The relation between load and the size of indentation can be correlated using Meyer's law, $P = k_1 d^m$ where k_1 is a constant and 'm' is the Meyer's index. The slope of $\log P$ versus $\log d$ (Fig. 8 (b)) gives the work hardening coefficient (m) and it was calculated to be 6.3 which indicates that 2A5CPC crystal belongs to soft material category.

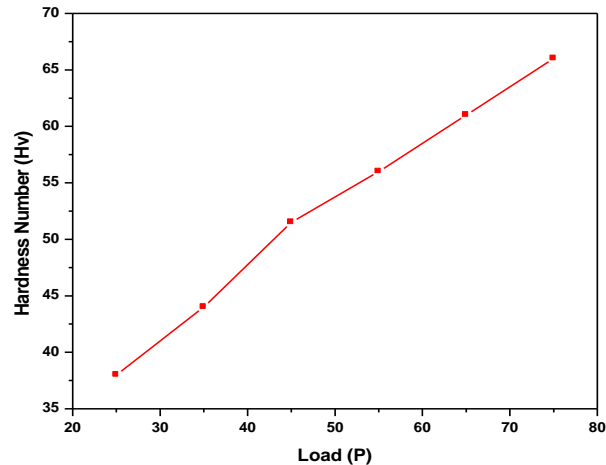


Fig. 8.(a) Variation of micro hardness number with load of 2A5CPC

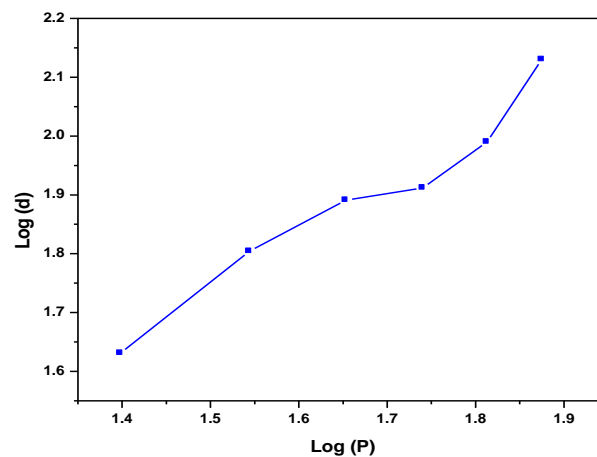


Fig.8. (b) Log (p) versus Log (d) of 2A5CPC

3.8SEM Analysis

The quality of the grown crystals can be inferred to some extent by observing the surface morphology of the cut and polished samples. The observation of the cut and lapped wafers by naked eye indicates that the crystals grown had large grains and inclusions[20]. The surface morphology of the sample was observed by the metallurgical optical microscope in the reflection mode. Metallax- II metallurgical microscope was used for this purpose. For experimental purpose, the transparent crystals were taken and cut into few mm for observing the surface morphology of the grown crystals. The SEM images of 2A5CPC at various magnifications are shown in Fig. 9. It was observed from the photographs the grown crystals have cracks and visible inclusions. The 2A5CPC crystals are well dispersing and most of the domain structures observed in various magnifications did not coalesce and they are lenticular in shape.

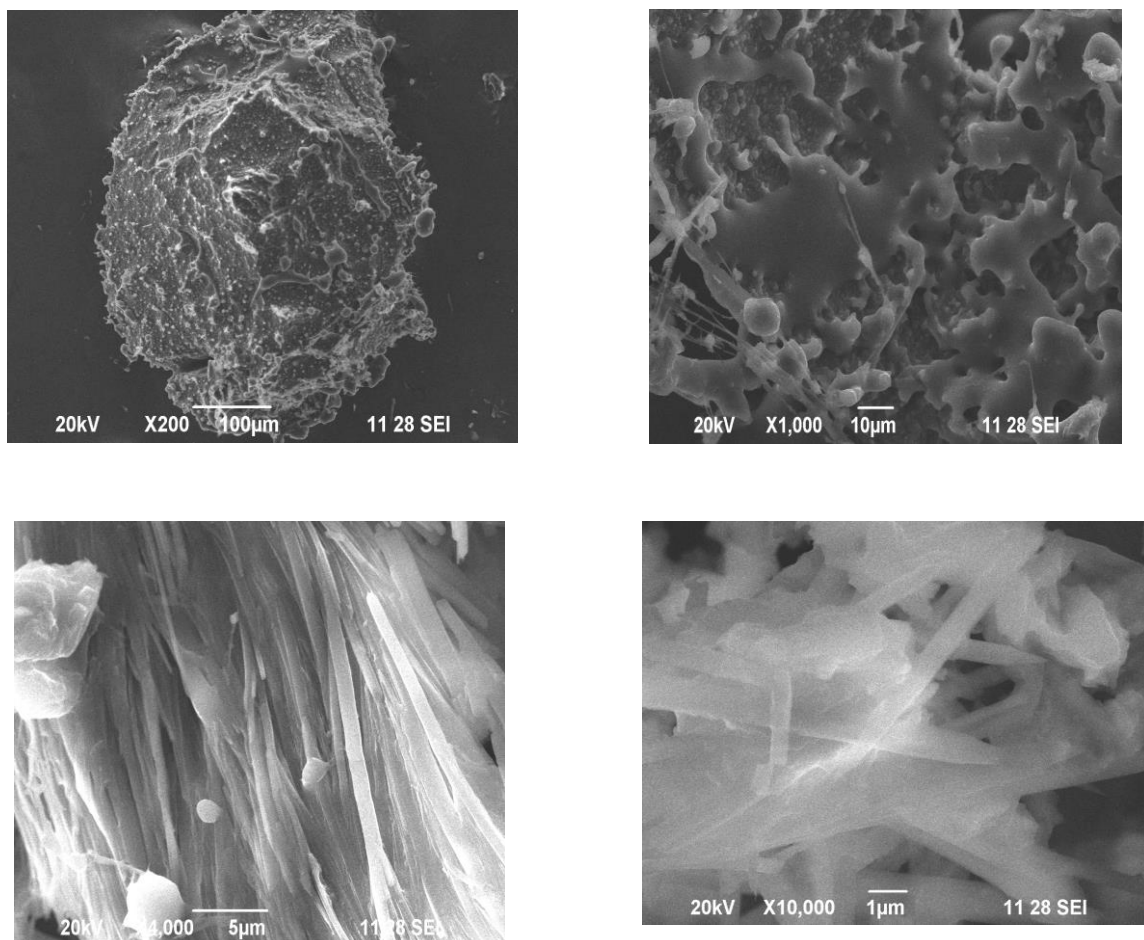


Fig. 9 SEM images of 2A5CPC at various magnifications

3.9 Energy dispersive analysis of X-ray

“The Energy Dispersive Analysis of X-rays” is an inevitable tool to estimate the semi quantitative chemical composition of crystals. The EDAX spectrum gives information about the chemical elements present in the sample, irrespective of their state of chemical combination of phases in which they exist, unlike the x-ray diffraction which discloses various compounds and phases present in the sample. Hence the EDAX is a much more rapid method of chemical analysis and is nondestructive. In the present investigation ‘Philips’ EM400 scanning electron microscope with an EDS attachment is used for the purpose of an elemental analysis by energy dispersion method. The energy spectrum of the grown crystal is shown in Fig. 10. The energy spectrum confirms the presence of 2- amino 5- chloropyridine and 2- picolinic acid. The elemental composition of the grown crystal is given in Table. 5.

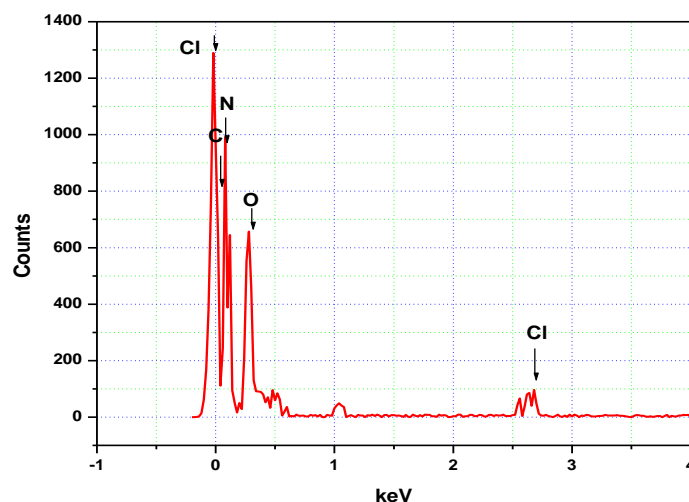


Fig.10 Energy dispersive X- ray analysis of 2A5CPC

Table. 5. EDAX analysis of 2A5CPC

Element	Spectral type	Element %	Atomic %
CK	ED	38.90	44.23
NK	ED	34.96	34.09
OK	ED	24.77	21.15
ClK	ED	1.37	0.53
Total		100	100

4. Conclusion

Single crystals of 2- amino - 5- chloropyridinium pyridine- 2- carboxylate monohydrate were successfully grown by the slow evaporation solution growth method and its structure is reported for the first time in the literature. The grown crystals have been confirmed using single crystal X-ray diffraction studies and it belongs to the monoclinic system with the space group $P2_1/c$. The presence of protons and carbons was confirmed by ^1H and ^{13}C NMR analyses. The modes of vibration of different functional groups present in the sample were identified by the FT-IR spectral analysis. The cut off wavelength of 2- amino - 5- chloropyridinium pyridine- 2- carboxylate monohydrate from the transmittance spectrum is 225nm and suggests the suitability of 2- amino - 5- chloropyridinium pyridine- 2- carboxylate monohydrate crystal for various optical applications. The grown crystals are transparent in the entire visible region. The results of dielectric measurements indicate that the dielectric constant and dielectric loss increases with the increase in temperature and it is due to the temperature variation of polarizability. In addition, the results obtained indicate that the grown crystal is a low dielectric constant material. From the mechanical measurements, it was observed that the hardness increases with increase of load and the material belongs to soft material category. The surface morphology of the grown crystals at various magnifications was studied in SEM analysis. The EDAX analysis reveals the presence of chemical elements in the grown crystal.

Supplementary information

The crystallographic data of $C_{11}H_{12}ClN_3O_3$ has been deposited with the Cambridge Crystallographic Data Centre [CCDC No. 1036880]. Copies of the data can be obtained free of charge at www.ccdc.cam.ac.uk/conts/retrieving.html [or from the Cambridge Crystallographic Data Centre (CCDC), 12 Union Road, Cambridge CB2 1EZ, UK; fax: +44 0 1223 336 033; email: deposit@ccdc.cam.ac.uk].

References

- [1] N. Ramamurthy, S. Dhanuskodi, M.V. Manjusha, J. Philip, *Opt. Mater.* **33**, 607 (2011).
- [2] G. Venkatesan, G. Anandha Babu, P. Ramasamy, A. Chandramohan, *J. Mol. Struct.* **1033**, 121 (2013).
- [3] R.W. Munn, C.N. Ironside, *Principles and Applications of Nonlinear Optical Materials*, Chapman & Hall, London, 1993.
- [4] M. Jose, R. Uthrakumar, A. Jeya Rajendran, S. Jerome Das, *Spectrochim. Acta A: Mol. N. Biomol. Spectrosc.* **86**, 495 (2012).
- [5] S. Lin, L. Li, J. Chen, Y. Chen, *J. Cryst. Growth* **249**, 341 (2003).
- [6] A. Datta, S.K. Pati, *J. Chem. Phys.* **118**, 8420 (2003).
- [7] S. C. Abrahams, J. M. Robertson *Acta Cryst.* **1**, 252 (1948).
- [8] J. Donhue, K. N. Trueblood *Acta Cryst.* **9**, 960 (1956).
- [9] W. Yang, L. Chen, S. Wang, *Inorg. Chem.* **40**, 507 (2001).
- [10] T. Jayanalina, G. Rajarajan, K. Boopathi, K. Sreevani, *J. Cryst. Growth* **426**, 9 (2015).
- [11] J. Zyss, R. Masse, M. Bagieu-Beucher, J.P. Levy, *Adv. Mater.* **5**, 120 (1993).
- [12] J. Zaccaro, B. Capelle, A. Ibanez, *J. Cryst. Growth* **180**, 229 (1997).
- [13] J. Pecaut, J.P. Levy, R. Masse, *J. Mater. Chem.* **3**, 999 (1993).
- [14] Bruker, APEX2 and SAINT-Plus, Bruker AXS Inc., Madison, Wisconsin, USA, 2004.
- [15] G.M. Sheldrick, *Acta Crystallogr., Sec. A: Found. Crystallography* **64**, 122 (2008).
- [16] F. Perron – Sierra, S.D. Dizier, M. Bertrand, A. Genton, G.C. Tucker, P. Casarsa, *Bioorg Med. Chem. Lett* **12**, 3291 (2002).
- [17] D. Xue, K. Kitamura, *Solid State Commun.* **122**, 541 (2002).
- [18] C. Balarew, R. Duhlev, *J. Solid State Chem.* **55**, 1 (1984).
- [19] N. Sundaraganesan, S. Ilakiamani, B. Anand, H. Saleem, B. Dominic Joshua, *Spectrochimica Acta Part A* **64**, 586 (2006).
- [20] S. Janarthanan, T. Kishore Kumar, S. Pandi, D. Prem Anand, *Indian J Pure & Appl Phys.* **47**, 332 (2009).